

“Click” Modification of Silica Surfaces and Glass Microfluidic Channels

Shaurya Prakash,[†] Timothy M. Long,^{†,‡} John C. Selby,[†] Jeffrey S. Moore,^{*,‡} and Mark A. Shannon^{*,†}

Department of Mechanical Science and Engineering and Department of Chemistry, University of Illinois at Urbana–Champaign, Urbana, Illinois 61801

This paper demonstrates a chemical surface modification method for covalent attachment of various polymers by using silane-based “click” chemistry on silica surfaces and within glass microchannels suitable for CE systems. Modified surfaces are characterized by contact angle measurements, X-ray photoelectron spectroscopy, and Fourier transform infrared-attenuated total reflection spectroscopy. Electroosmotic flow (EOF) measurements in modified and unmodified channels are provided. Spectroscopic and transport data show that various polymers can be covalently attached to glass surfaces with a measurable change in EOF.

Advances in microelectronic processing methods and microelectromechanical systems led to development of glass- or silica-coated silicon devices for “lab-on-chip” or micro-total analytical systems (μ -TAS).¹ Electrophoretic separations are one of the more common applications of these analytical microfluidic devices.^{2–4} Microchip capillary electrophoresis was initially developed in glass microchips toward the concept of μ -TAS.^{1,4} Glass remains the material of choice for some applications and commercial devices despite higher cost due to better optical clarity, well-understood surface chemistry, and advanced fabrication technologies adapted from the microelectronics industry in comparison to polymers.^{5–7} Applications for microfluidic chips include electrophoretic separations, DNA and protein analyses, PCR amplification, analytical chemistry applications such as protein extraction and purification, and fundamental study of fluid mechanics in confined channels at low Reynolds number flows.^{4–10}

Separation rates and resolutions within capillary electrophoretic (CE) systems can be enhanced^{11,12} when surface ζ potentials are uniform with minimum deviations from ideal pluglike flow. The ability to change surface chemistry within the micro- and nano-fluidic channels provides the ability to alter the effective surface charge and thus control the ζ potential. Uniform surface charges can assist in minimizing pressure-driven flows and subsequent deviation from pluglike flows.^{13–16} Thus, the ability to alter surface potential to produce desired electroosmotic flow (EOF) characteristics within a microchannel can be a powerful tool for a separations technologist. For CE systems, wall coatings can help improve electrophoretic separation reproducibility, reduce analyte–wall interactions, and provide greater control over EOF and device performance.^{16–20} Different methods have been used to control EOF in CE systems, including manipulation of buffer concentrations, addition of surfactants and surface-active materials to analyte solutions, application of radial electric fields, manipulating solution pH, and chemical modification of surfaces to alter ζ potential.¹⁸ The common link between all these methods is an attempt to control the interaction between the solution in the channel and the double layer at the channel wall surface.

Devices fabricated in glass, fused silica, or silica-coated silicon (Si/SiO₂) are convenient for exploring silane-based surface modification chemistries.^{21,22} Some of these chemistries can be extended to devices fabricated in polymers such as PMMA.²³ Among the chemical modification methods for altering channel wall properties, attachment of a polymer coating to a capillary was

* To whom correspondence should be addressed. E-mail: moore@scs.uiuc.edu; mshannon@uiuc.edu.

[†] Department of Mechanical Science and Engineering.

[‡] Department of Chemistry.

- (1) Manz, A.; Graber, N.; Widmer, H. M. *Sens. Actuators, B: Chem.* **1990**, *1*, 244–248.
- (2) Flachsbarth, B. R.; Wong, K.; Iannaccone, J. M.; Abante, E. N.; Vlach, R.; Rauchfuss, P. A.; Bohn, P. W.; Sweedler, J. V.; Shannon, M. A. *Lab Chip* **2006**, *6*, 667–674.
- (3) Prakash, S.; Yeom, J.; Shannon, M. A., Hilton Head Island, SC, Transducer Research Foundation, June 4–8, 2006; pp 102–103.
- (4) Seiler, K.; Harrison, D. J.; Manz, A. *Anal. Chem.* **1993**, *65*, 1481–1488.
- (5) Fan, Z. H.; Harrison, D. J. *Anal. Chem.* **1994**, *66*, 177–184.
- (6) Jacobson, S. C.; Hergenroder, R.; Koutny, L. B.; Ramsey, J. M. *Anal. Chem.* **1994**, *66*, 1114–1118.
- (7) Chen, L.; Ren, J. *Comb. Chem. High Throughput Screening* **2004**, *7*, 29–43.
- (8) Woolley, A. T.; Mathies, R. A. *Proc. Natl. Acad. Sci. U.S.A.* **1994**, *91*, 11348–11352.
- (9) Emrich, C. A.; Tian, H.; Medintz, I. L.; Mathies, R. A. *Anal. Chem.* **2002**, *74*, 5076–5083.

- (10) Ismagilov, R. F.; Stroock, A. D.; Kenis, P. J. A.; Whitesides, G.; Stone, H. A. *Appl. Phys. Lett.* **2000**, *76*, 2376–2378.
- (11) Reyes, D. R.; Iossifidis, D.; Auroux, P.-A.; Manz, A. *Anal. Chem.* **2002**, *74*, 2623–2636.
- (12) Herr, A. E.; Molho, J. J.; Santiago, J. G.; Mungal, M. G.; Kenny, T. W.; Garguilo, M. G. *Anal. Chem.* **2000**, *72*, 1053–1057.
- (13) Auroux, P.-A.; Iossifidis, D.; Reyes, D. R.; Manz, A. *Anal. Chem.* **2002**, *74*, 2637–2652.
- (14) Belder, D.; Ludwig, M. *Electrophoresis* **2003**, *24*, 3595–3606.
- (15) Kirby, B. J.; Hasselbrink, E. F., Jr. *Electrophoresis* **2004**, *25*, 187–202.
- (16) Vilcner, T.; Janasek, D.; Manz, A. *Anal. Chem.* **2004**, *76*, 3373–3386.
- (17) Doherty, E. A. S.; Meagher, R. J.; Albarghouthi, M. N.; Barron, A. E. *Electrophoresis* **2003**, *24*, 34–54.
- (18) Horvath, J.; Dolnik, V. *Electrophoresis* **2001**, *22*, 644–655.
- (19) Munro, N. J.; Hühmer, A. F. R.; Landers, J. P. *Anal. Chem.* **2001**, *73*, 1784–1794.
- (20) Prakash, S.; Long, T. M.; Wan, J.; Moore, J. S.; Shannon, M. A. ASME, Limerick, Ireland, June 19–21, 2006.
- (21) Breisch, S.; de Heij, B.; Lohr, M.; Stelzle, M. J. *Micromech. Microeng.* **2004**, *14*, 497–505.
- (22) Pesek, J. J.; Matyska, M. T. *J. Chromatogr., A* **1996**, *736*, 255–264.
- (23) Long, T. M.; Prakash, S.; Shannon, M. A.; Moore, J. S. *Langmuir* **2006**, *22*, 4104–4109.

first demonstrated two decades ago²⁴ by *in situ* polymerization of acrylamide for separation of proteins. Since then, several methods have been used for many different polymer coatings on capillary and microchannel surfaces. Researchers have modified microfluidic channel surfaces through *in situ* graft-polymerization of hydrogels or adsorption of polyelectrolyte layers within the channels.²⁵ However, these methods can have problems due to poor surface adhesion and desorption of the coating from the channel surface in addition to problems related to reproducibility of the polymer coating.¹⁸ In contrast, covalent attachment of preformed polymers as channel wall coatings is a promising path toward the goal of achieving a high degree of control on channel wall properties.^{14,16,18,19,26} Many different coatings have been reported in the literature for myriad applications. These include some covalently attached surface layers and many physisorbed polymer coatings. Examples include mono-, di-, and trichlorosilanes, ethoxy- and methoxysilanes, polymer coatings such as acrylamide-derived polymers, cellulose-derived polymers, poly(ethylene oxide) (PEO) and poly(ethylene glycol) (PEG),²⁶ poly(vinyl alcohol), oligourethanes, and poly(ethyleneimine) (PEI).²⁷ These coatings have been used to modify the surface ζ potential and provide control and tunability of EOF in addition to minimizing or eliminating analyte-wall interactions. Wetting characteristics of the channels, capillaries, or both are also changed.^{17–19} PEO or PEG is believed to coat surfaces by hydrogen bonding with the surface silanol groups. It was modestly effective at suppressing electroosmotic mobility at pH 7. Hydrophilicity of the coating is important for bioseparations as increased hydrophilicity reduces the analyte-wall interactions thereby increasing separation efficiency and improving resolution. However, the increased hydrophilicity also reduces the stability of the coating.¹⁹ This paper reports on the goal of chemically modifying glass microchannel surfaces by covalently attaching preformed polymers using well-developed silane chemistries²⁸ and “click”²⁹ reactions. This paper demonstrates a modular approach for surface attachment of terminally functionalized linear and dendritic polymers to glass microfluidic channels.

“Click” chemistry is defined as a class of robust and selective chemical reactions with high yields, tolerant to a variety of solvents (including water), functional groups, and air.²⁹ Among these, the previously known copper-catalyzed Huisgen cycloaddition of alkynes and azides is considered to be particularly useful for rapid and facile construction of combinatorial arrays²⁹ for drug discovery.³⁰ The reaction proceeds in aqueous solvents and in the presence of air to yield stable 1,2,3-triazoles. This reaction has been utilized for rapid and facile modification of surfaces.^{31–37}

Previous work includes the demonstrations of this chemistry to modify silica surfaces and silica gel,³⁵ gold electrodes,^{31,38} and single-wall carbon nanotubes.³⁹

The purpose of this paper is to develop and demonstrate a methodology for covalent attachment of preformed terminally functionalized linear and dendritic polymers to silica surfaces and glass microfluidic channels (Scheme 1a) to modify the surface and thus change the ζ potential by using well-known methods of “click” chemistry. As a consequence of the altered ζ potential, the EOF in channels can be changed in a systematic manner.

EXPERIMENTAL SECTION

Materials and Chemicals. Glass slides (Corning 2947) and cover glass (Premium No. 1, Fisher Scientific) were cleaned with acetone, isopropyl alcohol, and deionized (DI) water and then dried under a nitrogen stream. 11-Bromoundecyltrichlorosilane (BUTS; Gelest, Inc., Morrisville, PA) was used as received and was vapor deposited using a MVD100 system (Applied Microstructures, Inc., San Jose, CA) in a chamber held at 35 °C. Sodium azide, copper sulfate, sodium ascorbate, and *N,N*-dimethylformamide (DMF) were purchased from Sigma-Aldrich (Saint Louis, MO) and used without further purification. The terminal alkynes used for “click” modification were synthesized in-house, and information on synthesis methodology is available in the Supporting Information.

Silane Treatment. Surface modification was first tested on Si wafers with 1 μm of thermal oxide. BUTS was vapor deposited in a chamber held at 35 °C using a MVD100 system. BUTS was heated to 130 °C to generate sufficient vapor, the vapor injection pressure being maintained at 175 mTorr.

Nucleophilic Substitution. The bromo-terminated surface was used as the starting point for “click” modification by conversion to an azido-terminated surface through $\text{S}_{\text{N}}2$ nucleophilic substitution (Scheme 1a). The substitution reaction is carried out overnight by exposing the bromo-terminated substrates to a saturated solution of NaN_3 in DMF in a covered container. The sample was then rinsed with DMF followed by methanol and DI water before drying in a stream of N_2 .

“Click” Modification. For surface treatments, solutions of the alkyne-terminated polymers were prepared (5 or 10 mM) in either ethanol or methanol. The azido-terminated substrates were exposed to the polymer solutions for a minimum of 2 h in the presence of $\text{CuSO}_4 \cdot 5\text{H}_2\text{O}$ (0.1 mM) and sodium ascorbate (0.25–2 mol %). The samples were rinsed with copious amounts of water followed by a rinse in 1% v/v NH_4OH and DI water to remove excess copper.

Surface Characterization. All samples were characterized by water contact angle measurements, X-ray photoelectron spectroscopy (XPS),^{40,41} and Fourier transform infrared-attenuated total reflection spectroscopy (FT-IR-ATR).^{42,43} In addition, the glass microfluidic channels were characterized by measuring EOF⁴⁴ in

(24) Hjertén, S. *J. Chromatogr.* **1985**, *347*, 191–198.

(25) Uyama, Y.; Kato, K.; Ikada, Y. *Adv. Polym. Sci.* **1998**, *137*, 1–39.

(26) Belder, D.; Hussman, H.; Warnke, J. *Electrophoresis* **2001**, *22*, 666–672.

(27) Erim, F. B.; Cifuentes, A.; Poppe, H.; Kraak, J. C. *J. Chromatogr., A* **1995**, *708*, 356–361.

(28) Ulman, A. *Chem. Rev.* **1996**, *96*, 1533–1554.

(29) Kolb, H. C.; Finn, M. G.; Sharpless, K. B. *Angew. Chem., Int. Ed. Engl.* **2001**, *40*, 2004–2021.

(30) Fazio, F.; Bryan, M. C.; Blixt, O.; Paulson, J. C.; Wong, C.-H. *J. Am. Chem. Soc.* **2002**, *124*, 14397–14402.

(31) Collman, J. P.; Devaraj, N. K.; Chidsey, C. E. D. *Langmuir* **2004**, *20*, 1051–1053.

(32) Collman, J. P.; Devaraj, N. K.; Eberspacher, T. P. A.; Chidsey, C. E. D. *Langmuir* **2006**, *22*, 2457–2464.

(33) Guo, Z.; Lei, A.; Liang, X.; Xu, Q. *Chem. Commun.* **2006**.

(34) Lin, P.-C.; Ueng, S.-H.; Tseng, M.-C.; Ko, J.-L.; Huang, K.-T.; Adak, A. K.; Lin, C.-C. *Angew. Chem., Int. Ed.* **2006**, *45*, 4286–4290.

(35) Lummerstorfer, T.; Hoffman, H. *J. Phys. Chem. B* **2004**, *108*, 3963–3966.

(36) Seo, T. S.; Bai, X.; Ruparel, H.; Li, Z.; Turro, N. J.; Ju, J. *Proc. Natl. Acad. Sci. U.S.A.* **2004**, *101*, 5488–5493.

(37) Wollman, E. W.; Kang, D.; Frisbie, C. D.; Lorkovic, I. M.; Wrighton, M. S. *J. Am. Chem. Soc.* **1994**, *116*, 4395–4404.

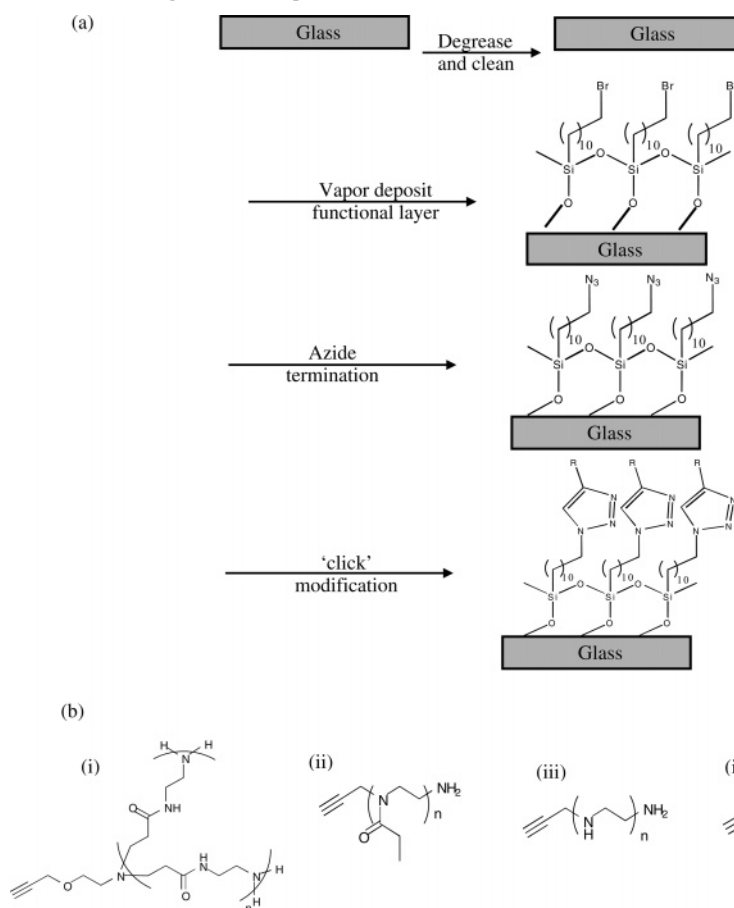
(38) Lee, J. K.; Chi, Y. S.; Choi, I. S. *Langmuir* **2004**, *20*, 3844–3847.

(39) Li, H.; Cheng, F.; Duft, A. M.; Adronov, A. *J. Am. Chem. Soc.* **2005**, *127*, 14518–14524.

(40) Loh, F. C.; Tan, K. L.; Kang, E. T.; Neoh, K. G.; Pun, M. Y. *J. Vac. Sci. Technol., A* **1994**, *12*, 2705–2710.

(41) Wagner, C. D. *J. Electron Spectrosc. Relat. Phenom.* **1983**, *32*, 99–102.

Scheme 1. (a) Modular Scheme for Silane-Based “Click” Modification of Glass Surfaces.^a (b) Example Structures of Different Coatings Developed for “Click” Modification of Glass Surfaces^b



^a An alkyltrichlorosilane is used to set up the modular reaction by providing a site for nucleophilic substitution. The “click” modification attaches desired functionality to the glass surface. ^b (i) An example of the PAMAM dendrimers. $n = 0-3$ were synthesized. (ii) PEO_x; (iii) PEI; and (iv) m-PEG.

modified and unmodified channels to determine the effect, if any, of the adherent surface layers. Contact angles were measured on a Rame-Hart (Mountain Lake, NJ) XRL C.A. Goniometer (model 100-00) and were measured as the advancing angle of a sessile drop of distilled (Millipore, 18 MΩ) water. Each sample was measured at three to five locations on the deposited organic film to check for uniformity. XPS spectra were recorded for functionalized surfaces by a Kratos Axis Ultra X-ray spectrometer (Al K α radiation, 15 kV, 225 W). Measurements were done at pass energies of 160 eV for the survey scans. The detail scans were performed at pass energies of 40 eV with a beam spot size of 0.3×0.7 mm. Two scans are collected for each survey and 10 scans are collected for the detail scans for each sample tested. The base pressure for all measurements was no higher than 5×10^{-8} Torr. The samples were attached to the sample holder with UHV-compatible Cu tape. FT-IR-ATR spectra were collected on a Nicolet Magna-IR 750 spectrometer (Madison, WI) with a Harrick (Ossining, NY) Seagull reflectance accessory by placing the sample in contact with a Ge hemisphere ($n = 4.0$).

Device Fabrication. Glass microfluidic devices were made by patterning a single channel on Corning 2947 microscope slides

by using AZ1518 (Clariant, Inc.) as the photoresist (PR). AP8000 (Dow Chemicals) was used as the adhesion promoter for the PR layer, which was later used as the etch mask.²⁰ The patterned microscope slides were exposed to a 4:1 solution of DI water and NH₄F/HF (BHF) for 20 min with gentle agitation. Following glass etching, the PR was stripped using acetone and the devices were rinsed with DI water and dried in a stream of N₂. Using PR as an etch mask leads to a larger undercut in comparison to using a metal mask. This problem was resolved by allowing for the undercut in mask design. The final dimensions of the devices were 30 mm long channels with 3 mm diameter reservoirs. The channels were 100 ± 20 μ m wide and 15 ± 5 μ m deep. The dimensions were verified by profilometry (Tencor P10 profilometer). The channels were sealed with a cover glass slide with 4 mm holes drilled in the cover glass. The two glass slides were bonded together by contact printing with a commercial adhesive² transferred from a PDMS master and thermally bonded at 130 °C and a contact force of 3000 N in the EV501 anodic bonder (EV Inc.). Following bonding, the assembled devices were cured for at least 24 h in a conventional vacuum oven at 95 °C.

EOF Measurements. EOF characterization was performed on both untreated and surface-modified glass devices. At least two devices of each type were tested multiple times. The reported data are the average of all measurements with associated standard

(42) Lummerstorfer, T.; Hoffman, H. *Langmuir* **2004**, *20*, 6542–6545.

(43) Rochat, N.; Chabli, A.; Bertin, F.; Olivier, M.; Vergaud, C.; Mur, P. *J. Appl. Phys.* **2002**, *91*, 5029–5034.

(44) Huang, X.; Gordon, M. J.; Zare, R. N. *Anal. Chem.* **1988**, *60*, 1837–1838.

deviations. EOF measurements were performed in two steps. First, the reservoirs and the channels were filled with a 10 mM phosphate buffer saline (PBS) of pH 7.2–7.4. Pt wires were used as electrodes to establish electrical contact with the PBS in the reservoirs. A current–voltage (I – V) curve was generated to check for electrical continuity and the onset of Joule heating. For all devices tested, the onset of Joule heating was ~300–350 V. Second, one reservoir was replaced with 5 mM PBS buffer at pH 7.2–7.4, and current was recorded for the 5 mM buffer moving to the 10 mM side for an applied bias of 100 V across the channel with respect to ground. Current was recorded as a function of time as the 5 mM buffer replaced the 10 mM buffer solution in the channel.⁴³ EOF values were calculated from these measurements by using an asymptotic approach.^{23,44} In addition, all devices were checked visually under a Leica fluorescence microscope (model DMIRE2, Leica Microsystems Wetzlar GmbH) to ensure that the channels were completely filled and no bubbles were trapped in the channel. Flow imaging measurements were also carried out using fluorescein as an indicator dye to qualitatively determine the effect of applied channel wall coatings on ionic transport within the microfluidic channels. All current and voltage measurements were done on a HP3457A multimeter. A Bertan model 215 power supply was used as the high-voltage power supply for these experiments.

RESULTS AND DISCUSSION

Surface Coatings. For this paper, four categories of surface coatings were developed. These are different generations of poly-(amido amine) (PAMAM) dendrimers,⁴⁵ linear m-PEG, PEI, and poly(2-ethylloxazoline) (PEOX) of different molecular weights to evaluate degrees of surface coverage and potential effect on EOF in modified glass channels. Scheme 1b shows an example of each type of polymer that was synthesized with terminal alkynes for “click” modification. The versatility and scope of several different types of coatings and materials are evident from the literature cited above and the data presented in Table 1.

Contact Angle. Contact angle was measured to obtain a preliminary estimate of the relative hydrophobicity of each sample as the surface energies change after modification with respect to clean glass surfaces. The results are summarized in Table 1. Values from literature, where available, are also listed in Table 1. It can be seen from Table 1 that the bromo- and azido-terminated surfaces have values similar to those presented in the literature. The amine-terminated polymers tend to have a wide range of values from 30 to 63°. ^{46–48} The values measured for the surface coatings in this paper fall within the range of values already cited in the literature (Table 1).

XPS. After modification, surfaces were characterized by XPS to obtain chemical composition and electronic structure information of the adherent layers. XPS spectra were collected at each stage of the surface modification process (Scheme 1a) beginning with the silanization of the SiO₂, followed by the azide nucleophilic

Table 1. Contact Angle Data for Glass Surfaces after Modification

surface	contact angle (deg) ^a	lit. contact angle (deg)
clean SiOH	2	2
Br-(CH ₂) ₁₁ -	85	84 ⁵¹
N ₃ -(CH ₂) ₁₁ -	77	77–84 ^{52,53}
click functionalization		
CF ₃ (CF ₂) ₈ CH ₂ OCH ₂ CCH	123	> 115
H(OCH ₂ CH ₂) ₆ OCH ₂ CCH PEG (6)	39	23–50
m-PEG 750	42	
m-PEG 2000	33	
G0.0 dendrimer	35	
G0.5 dendrimer	57	
G1.0 dendrimer	53	30–63 ^b
G1.5 dendrimer ^c	57	
G2.0 dendrimer ^c	57	
G2.5 dendrimer ^c	59	
G3.0 dendrimer ^c	48	
PEOX-10 (1000)	45	
PEOX-25 (2500)	42	
PEOX-50 (5000)	41	
PEI ^d	33	

^a Least count on goniometer was 1°. ^b Contact angle reported in literature for large variety of dendrimer generations, see text for references. ^c Incomplete “click” coverage, some azide remains due to large footprint. ^d May require higher catalyst loadings.

substitution, and finally the “click” functionalization of the surfaces. Figure 1 shows a sequence of representative XPS data for the linear PEG layer and G1.0 PAMAM dendrimer on the surface. It can be seen from Figure 1a that the characteristic bromo peak appears at ~70 eV for the Br (3d) electronic state, indicating the successful silanization of SiO₂ with BUTS. Following silanization, the bromo group was substituted with an azido functional group as mentioned previously. Figure 1b shows the absence of the Br (3d) peak and a reduction in intensity of the Br (3p) peak following reaction with sodium azide. In addition, a strong nitrogen signal is detected at ~400 eV, and on performing a detailed scan, the characteristic azide double-peak structure is observed as shown in the inset to Figure 1b. The double-peak structure is indicative of the azide as the smaller peak is seen at 404.1 eV and the larger peak is seen at 400 eV, in agreement with previous results for azide peak location.^{37,49,50} Even though the ratio of areas of the two peaks is not exactly 1:2 as expected for surface azides, the difference in areas can be attributed to the well-known degradation of the middle nitrogen due to prolonged scanning.⁵⁰ The XPS scans for the surface azide groups lasted for almost 3 h. Continuing with the “click” modification, a six-carbon-long linear PEG and the G1.0 PAMAM dendrimer (Figure 1c,d) are attached to the SiO₂ surface. XPS analysis of the modified surfaces shows characteristic peaks for both of these polymers. The nitrogen peak

(45) Wu, P.; Malkoch, M.; Hunt, J. N.; Vestberg, R.; Kaltgrad, E.; Finn, M. G.; Fokin, V. V.; Sharpless, K. B.; Hawker, C. J. *Chem. Commun.* **2005**, 5775–5777.

(46) Kohli, N.; Dvornic, P. R.; Kaganove, S. N.; Worden, R. M.; Lee, I. *Macromol. Rapid Commun.* **2004**, *25*, 935–941.

(47) Tokuhisa, H.; Zhao, M.; Baker, L. A.; Phan, V. T.; Dermody, D. L.; Garcia, M. E.; Peez, R. F.; Crooks, R. M.; Mayer, T. M. *J. Am. Chem. Soc.* **1998**, *120*, 4492–4501.

(48) Yam, C. M.; Deluge, M.; Tang, D.; Kumar, A.; Cai, C. *J. Colloid Interface Sci.* **2006**, *296*, 118–130.

(49) Sano, M.; Wada, M.; Miyamoto, A.; Yoshimura, S. *Thin Solid Films* **1996**, *284–285*, 249–251.

(50) Schulze, R. K.; Boyd, D. C.; Evans, J. F.; Gladfelter, W. L. *J. Vac. Sci. Technol., A* **1990**, *8*, 2338–2343.

(51) Faucheux, N.; Schweiss, R.; Lutzow, K.; Werner, C.; Groth, T. *Biomaterials* **2004**, *25*, 2721–2730.

(52) Fryxell, G. E.; Rieke, P. C.; Wood, L. L.; Engelhard, M. H.; Williford, R. E.; Graff, G. L.; Campbell, A. A.; Wiacek, R. J.; Lee, L.; Halverson, A. *Langmuir* **1996**, *12*, 5064–5075.

(53) Heise, A.; Stamm, M.; Rauscher, M.; Duschner, H.; Menzel, H. *Thin Solid Films* **1998**, *327–329*, 199–203.

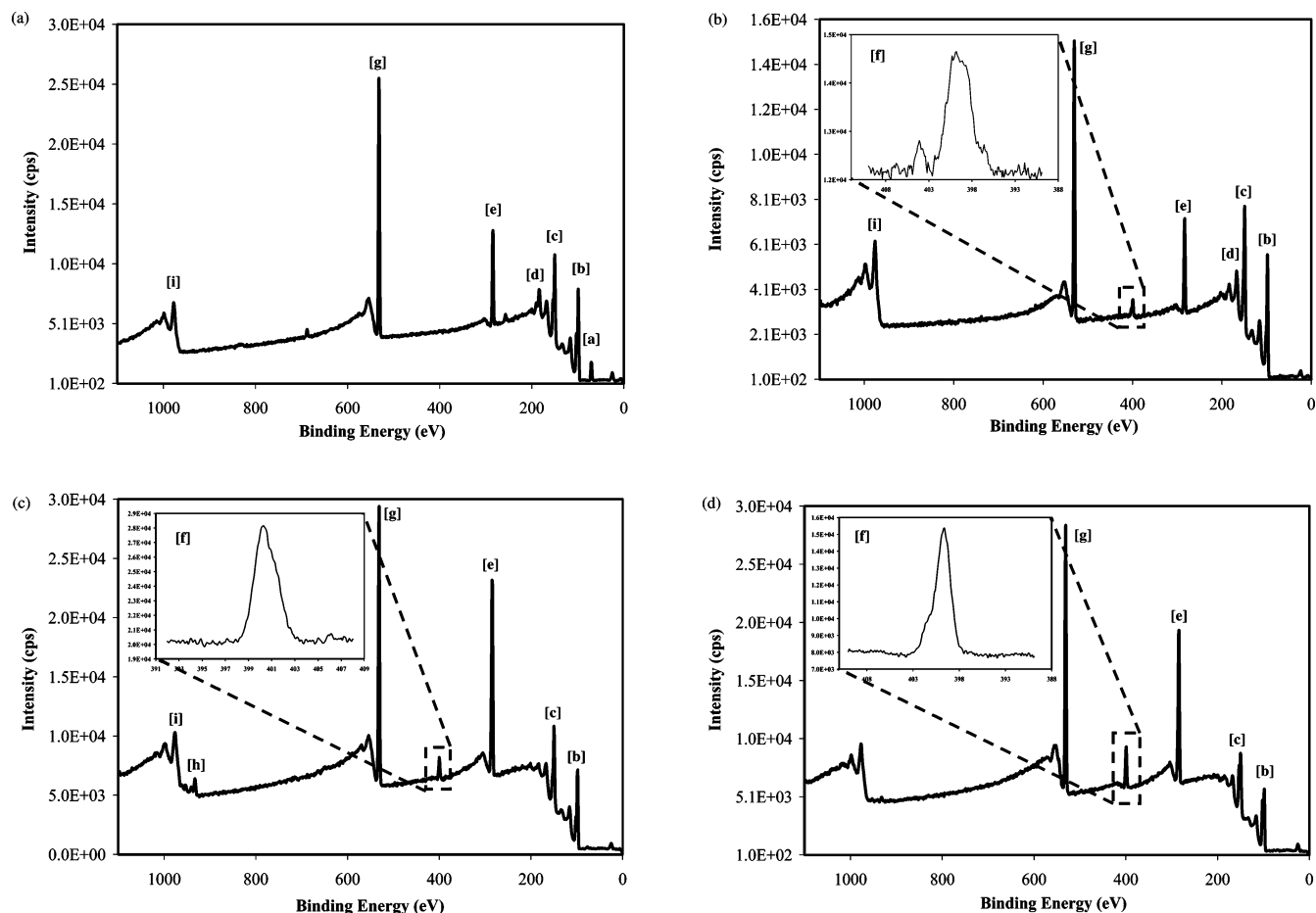


Figure 1. XPS spectra for “click” modification of glass. (a) Silanization of SiO₂, where characteristic Br peaks are seen. (b) Azide substitution of Br; the inset shows the typical azide double-peak structure. The Br (3d) peak is not seen and the Br (3p) peak has a relatively low intensity. (c) PEG(6) “click” functionalization is shown. The double-peak structure characteristic of the azide is no longer seen along with an increase in the C (1s) peak intensity and some Cu (2p) incorporation in the PEG(6) surface coating. The nitrogen peak is representative of triazole formation. (d) G1.0 PAMAM dendrimer coating is demonstrated here. Again, the azide double-peak structure is not seen, and the nitrogen peak is representative of the triazole formation. Peaks: [a] Br [3d], [b] Si [2s], [c] Si [2p], [d] Br [3p], [e] C [1s], [f] N [1s], [g] O [1s], [h] Cu [2p], and [i] O (Auger).

in the vicinity of 400 eV is observed with a marked difference in the peak shape. The characteristic double peak of the azide group is no longer observed, and the single broad peak is characteristic of the 1,2,3-triazole formed during the cycloaddition “click” reaction. Further, an increase in the intensity of the carbon peaks (~288 eV) is observed, indicating the presence of additional carbon on the surface. PEG coatings can have the Cu catalyst incorporated in them, as shown by the small Cu (2p) peak observed near 932 eV. The incorporated Cu can be removed by rinsing the sample in an aqueous 1% v/v NH₄OH after the “click” modification. Figure S1 (Supporting Information) shows the PEG(6) XPS spectra after rinsing with aqueous NH₄OH. Figure 1d shows the spectrum for the G1.0 PAMAM dendrimer. Again, the characteristic shape of the azide peak is no longer observed, but a single broad peak is characteristic of the 1,2,3-triazole formation as suggested by the XPS data. The peak near 980 eV seen in Figure 1 is due to the Auger signal from oxygen.

FT-IR-ATR. IR spectra were collected for modified surfaces with an ATR attachment to determine the chemical composition of the surfaces in question and to confirm “click” modification of SiO₂ surfaces through certain fingerprint regions. These data complement the contact angle and XPS measurements, providing strong evidence in support of desired surface modification. The

spectra for the azide functionalized Si/SiO₂ surfaces can be seen in Figure 2a. Spectra for silanized (with BUTS) glass surfaces are not shown as that chemistry is well-developed. It can be seen from Figure 2a that the surface azide shows a diagnostic fingerprint near 2100 cm⁻¹. The FT-IR-ATR data along with the XPS data confirm the presence of surface azide groups. After “click” modification, the absence of this identifying peak is taken as evidence for a successful “click” modification. Figure 2b shows the ATR spectra for the G1.0, G1.5, and G2.5 PAMAM dendrimer, and Figure 2c shows the ATR spectra for the PEG(6)-functionalized Si/SiO₂ surface. It can be observed from Figure 2b and c that the characteristic azide peak near 2100 cm⁻¹ is no longer detectable for the G1.0 and PEG(6) surfaces, indicating successful “click” functionalization. The insets in Figure 2b and c show the structure for the G1.0 PAMAM terminal alkyne and the PEG(6) terminal alkyne that were attached to the surfaces.

One criterion considered for comparing polymer coatings was the possible differences in surface coverage between the dendritic structures and the linear polymers. This comparison was performed by considering the FT-IR-ATR spectra for advanced generation ($n > 1.5$) PAMAM dendrimers to linear polymers m-PEG ($M_n \sim 750$) and PEOX ($n = 25$, Scheme 1b) as a representative case. It can be seen from Figure 2b that for the

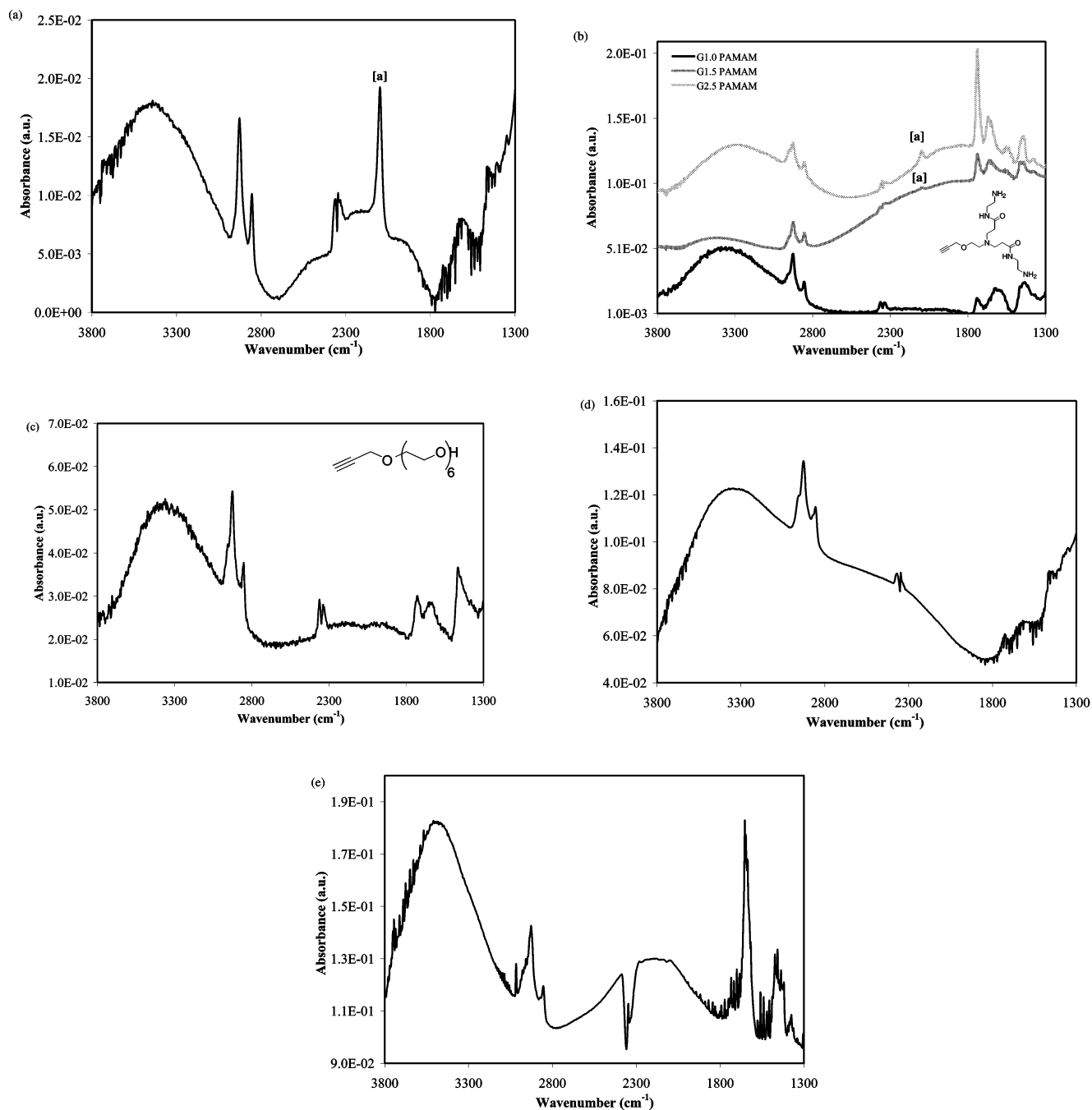


Figure 2. FT-IR-ATR spectra for “click” modification of glass. (a) Spectrum shows an azide-functionalized Si/SiO₂ surface. The characteristic azide peak is observed near 2100 cm⁻¹. (b) G1.0 PAMAM dendrimer spectrum on Si/SiO₂. The dendrimer with the terminal alkyne used for “click” modification is shown in the inset. The characteristic azide peak is not seen. (c) PEG(6) spectrum on Si/SiO₂ is observed and the azide peak is not seen. The terminal alkyne used for “click” modification is shown in the inset for (b) and (c). Various surface coatings on Si/SiO₂ compared using FT-IR-ATR. (d) G1.5, and (e) G2.5 PAMAM with residual azide (peak a near 2100 cm⁻¹) after “click” modification. (f) m-PEG (*M_n* ~750). (g) PEOX-25. In both (b) and (c), no residual azide is seen. Diagnostic peak, [a] azide.

G1.5 and G2.5 PAMAM dendrimers some residual azide signal is detected after “click” modification, indicating partial coverage or incomplete transformation of the azide to 1,2,3-triazole. Further, the relative IR signal intensity between G1.5 and G2.5 shows a stronger residual azide signal from the G2.5 surface coating. This stronger azide signal is most likely on account of the large footprint of the higher generation tree-like PAMAM dendrimers. On the other hand, linear polymers such as m-PEG (750) and PEOX-25 (Figure 2d and e) do not show any residual azide signal,

indicating complete utilization of the surface azides in the cycloaddition reaction.

EOF Characterization. The covalently bound surface polymer layers were characterized as part of a simple single-channel microfluidic device.²⁰ The goal of these measurements was to estimate the electroosmotic velocity in surface-modified microchannels. Changes in EOF in comparison to the untreated or bare glass microchannels are attributed to the applied surface coatings. Table 2 summarizes the EOF data for some of the coatings tested.

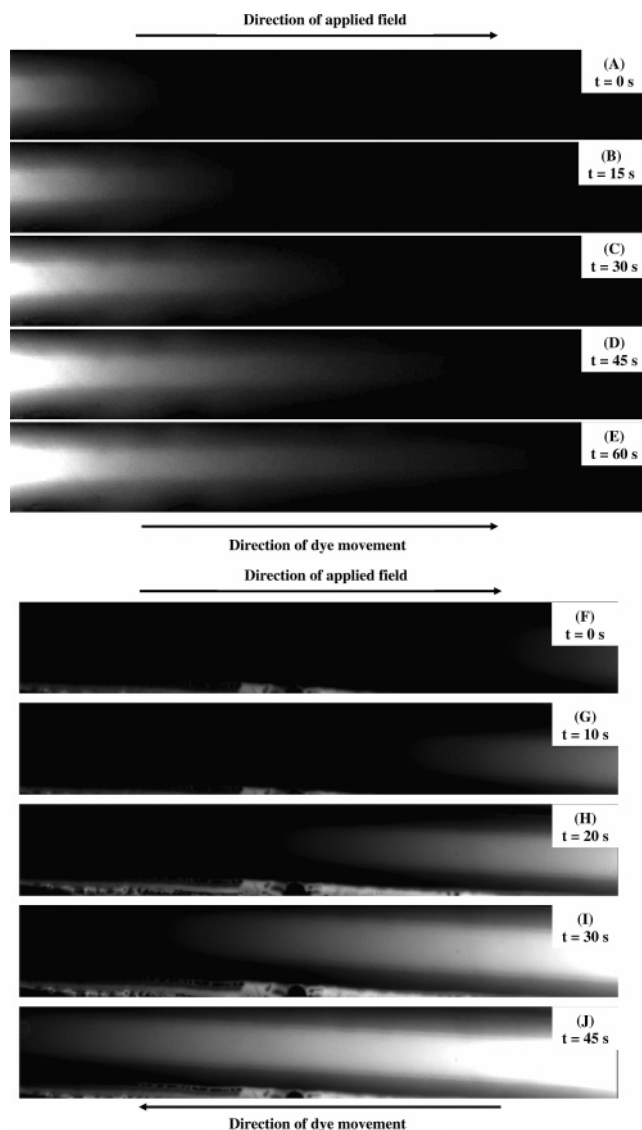


Figure 3. Sequence of time-elased images depicting flow imaging. For a negatively charged channel wall (BUTS), it is seen that the dye moves in the same direction as the applied field as seen in images A–E and for a positively charged surface (G0.0 PAMAM) the dye moves in the direction opposite to the applied field as seen images F–J. Fluorescein (1 mM) is used as the indicator dye, and the applied voltage for imaging is 150 V with respect to ground. The channel is filled with the 10 mM solution of PBS at pH of ~ 7 .

Table 2. Summary of EOF Data

S. No.	surface	measured EOF ($\text{cm}^2/\text{V}\cdot\text{s}$) ^a
1	bare glass	$4.6 \times 10^{-4} \pm 3.6 \times 10^{-5}$
2	BUTS coated	$5.0 \times 10^{-4} \pm 2.9 \times 10^{-5}$
3	azide	$5.3 \times 10^{-4} \pm 6.6 \times 10^{-5}$
4	G0.0 PAMAM	$-4.1 \times 10^{-4} \pm 2.7 \times 10^{-5}$

^a Uncertainty in applied voltage is ± 1 V, in measured time is ± 10 s, and in the length of the channel is a maximum of ± 3 mm.

Table 2 shows that the application of surface coatings also affects the effective surface charge. For instance, the PAMAM dendrimer coatings present an amine-terminated surface that at neutral pH (here 7.2 to 7.4) has a positive charge due to protonation. This

positive charge is in contrast to the normally negatively charged bare glass surfaces at similar pH. Thus, the expected EOF is opposite to that for a bare glass surface or a BUTS-coated surface. The opposite direction of EOF is qualitatively verified by flow imaging done using a negatively charged dye (fluorescein) in a 10 mM PBS-filled channel as shown in Figure 3. One BUTS-coated channel and one G0.0 PAMAM-coated channel were compared, and the fluorescence images indicate that the dye flow is in the opposite direction for the same applied field in the two channels. In Figure 3, the time elapsed images A–E show that for a negatively charged channel wall the indicator dye moves in the direction of the applied electric field; however, for a positively charged surface as in images F–J, the indicator dye is seen to move in a direction opposite to that of the applied electric field. The observed change in direction of the flow for the indicator dye is attributed to the change in surface charge due to the applied “click” coatings. The negative sign in Table 2 reflects the fact that the surface charge is opposite to that of bare glass. In comparison to the bare glass channels, the measured EOF for a G0.0 PAMAM-coated channel is lower by $\sim 11\%$ in the opposite direction. Furthermore, an azide-coated surface shows an increase of almost 15% in measured EOF in contrast to the bare glass channels. Thus, the use of various “click” coatings can either increase or reverse the EOF within microfluidic channels.

CONCLUSIONS

In this work, the application of “click” chemistry for covalent attachment of preformed terminally functionalized linear and dendritic polymers to glass microfluidic channels has been demonstrated. The surface modification approach demonstrated here relies on silane chemistry as the starting step. Thus, this method can also be used for surfaces such as fused silica or silica-coated silicon in addition to glass. This chemical surface modification scheme provides a methodology to change the ζ potentials thereby altering the EOF within the microfluidic channels in a systematic manner.

ACKNOWLEDGMENT

The authors thank the National Science Foundation for financial support for the current research through the Center for Nano-Chemical-Electrical-Mechanical Manufacturing Systems (Nano-CEMMS) under DMI-0328162 and the Science and Technology Center of Advanced Materials for the Purification of Water with Systems (WaterCAMPWS) under the agreement CTS-0120978. XPS measurements were carried out in the Center for Microanalysis of Materials, University of Illinois, which is partially supported by the U.S. Department of Energy under grant DEFG02-91-ER45439. We thank Dr. Richard Haasch for his assistance in obtaining XPS data and Jonathan Wan for help with fabricating devices. The authors are grateful to Kachuen Wong for help with flow imaging experiments.

SUPPORTING INFORMATION AVAILABLE

Additional information as noted in text. This material is available free of charge via the Internet at <http://pubs.acs.org>.

Received for review September 27, 2006. Accepted November 7, 2006.

AC061824N